dB/m. But calcite is preferable since the net gain (9.9857 dB/m) is better than with titania (7.4596 dB/m). This is so because it can be shown that the loss factor is minimized around $\bar{\epsilon}_r = 3$, a fact true for isotropic case also [2]. It infers that a material with $\bar{\epsilon}_r \simeq 3$ and $a \simeq 2$ is most suitable for best output.

References

[1] N. S. Kapany and J. J. Burke, *Optical Waveguides*. New York: Academic Press, 1972, pp. 293–318.
[2] E. A. J. Marcatili and R. A. Schmeltzer, "Hollow metallic and dielectric waveguides for long distance optical transmission and lasers," *Bell Syst. Tech. J.*, vol. 43, pp. 1783–1809, July 1964.

Toroidal Resonator with a Conducting Separating Wall

RUDOLF DEUTSCH

***Abstract*—The exact solution of Maxwell's equations for electromagnetic waves in toroidal resonators with a separating wall was obtained. The components of the intensities of the electric and magnetic fields, the charge densities on the toroidal surface and on the separating wall, the magnetic field lines, and the dispersion relation were determined. Both the empty torus and the coaxial torus were studied. A general method to determine in an easy way the magnetic field lines from the structure of the Hertz vector is given.**

I. Introduction

IT WAS RECENTLY shown [1]–[3] that the vectorial Helmholtz equation for electromagnetic waves in toroidal coordinates can be reduced to the scalar Helmholtz equation, and solutions of this equation for some cases important in electronics and in plasma physics were obtained. It is possible to get an exact solution with the periodicity of 4π [2]. This corresponds to an empty or coaxial torus containing a conducting separating wall (Fig. 3). In this paper, we shall study this solution in detail.

In the first part of the paper, we show that it is possible to introduce a generating function, related to the Cartesian components of the Hertz vector, and this function describes the magnetic surfaces of the stationary waves. This provides a general, easy method to construct the magnetic field lines. A series of examples of magnetic surfaces are given.

In the second part, we formulate the generating function for the exact solution with periodicity 4π and we describe the electromagnetic field in the resonators with a separating wall. The components of the electric and magnetic field's intensities, the magnetic field lines, and the charge densities on the conducting toroidal surface and on the separating wall are determined. Both the empty torus and the coaxial torus are studied.

In the third part of the paper, some particular examples are described.

II. The Structure of the Magnetic Field of the Stationary Waves

The intensity of the magnetic field can be expressed through the Hertz vector using the well-known relation

$$\vec{B} = i\omega\epsilon_0\mu_0 \operatorname{curl} \vec{P}. \tag{1}$$

Writing the differential equations for the magnetic field lines and inserting the field components from (1), we get, for toroidal systems, the following equations:

$$\begin{aligned} dP_\rho &= \frac{\partial P_\rho}{\partial \rho}\, d\rho + \frac{\partial(\rho P_\theta)}{\partial \rho}\, d\theta + \frac{\partial}{\partial \rho}(1-\rho\cos\theta)P_\phi\, d\phi \\ d(\rho P_\theta) &= \frac{\partial P_\rho}{\partial \theta}\, d\rho + \frac{\partial(\rho P_\theta)}{\partial \theta}\, d\theta + \frac{\partial}{\partial \theta}(1-\rho\cos\theta)P_\phi\, d\phi \\ d\left[(1-\rho\cos\theta)P_\phi\right] &= \frac{\partial P_\rho}{\partial \phi}\, d\rho + \frac{\partial(\rho P_\theta)}{\partial \phi}\, d\theta + \frac{\partial}{\partial \phi}(1-\rho\cos\theta)P_\phi\, d\phi \end{aligned} \tag{2}$$

where ρ, θ, and ϕ are the toroidal coordinates.

In the case of the electromagnetic waves, the components of the Hertz vector can be expressed through a

Manuscript received October 11, 1977; revised April 21, 1978.
The author is with the Institut für Theoretische Physik, Universität Innsbruck, Innsbruck, Austria.

0018-9480/79/0200-0172$00.75 ©1979 IEEE

function f, which is a solution of the scalar Helmholtz equation in toroidal coordinates. As it was shown in [1] and [2], three different toroidal eigenmodes can be defined through the Cartesian components of the Hertz vector in the following way:

$$1)\ P_x^a = A_1 f \qquad P_y^a = P_z^a = 0$$

$$2)\ P_x^b = 0 \qquad P_y^b = A_2 f \qquad P_z^b = 0$$

$$3)\ P_x^c = P_y^c = 0 \qquad P_z^c = A_3 f.$$

The corresponding toroidal components are

$$1)\ P_\rho^a = -A_1 f \cos\theta \cos\phi \qquad P_\theta^a = A_1 f \sin\theta \cos\phi$$
$$P_\phi^a = -A_1 f \sin\phi$$

$$2)\ P_\rho^b = -A_2 f \cos\theta \sin\phi \qquad P_\theta^b = A_2 f \sin\theta \sin\phi$$
$$P_\phi^b = A_2 f \cos\phi$$

$$3)\ P_\rho^c = A_3 f \sin\theta \qquad P_\theta^c = A_3 f \cos\theta \qquad P_\phi^c = 0 \tag{3}$$

(A_1, A_2, and A_3 are arbitrary constants).

The general form of the Hertz vector, which can be obtained from a single generating function, is the superposition of the defined three eigenvectors:

$$\vec{P} = \vec{P}^a + \vec{P}^b + \vec{P}^c. \tag{4}$$

Inserting in (2), we get the following system of equations:

$$P_\rho d\ln f = \frac{\partial f}{\partial \rho}\, du$$

$$P_\theta d\ln f = \frac{1}{\rho}\frac{\partial f}{\partial \theta}\, du \tag{5}$$

$$P_\phi d\ln f = \frac{1}{1-\rho\cos\theta}\frac{\partial f}{\partial \phi}\, du.$$

P_ρ, P_θ, and P_ϕ are the components of the vector $\vec{P}$ given by (4), and $u = A_1 x + A_2 y + A_3 z$ where $x = (1-\rho\cos\theta)\cdot\cos\phi$, $y = (1-\rho\cos\theta)\sin\phi$, and $z = \rho\sin\theta$.

From (1) results that $\vec{P}$ cannot be represented as a gradient of any function. Therefore, the only solution of system (5) is the trivial one

$$d\ln f = 0$$

$$du = 0. \tag{6}$$

Hence, the magnetic field lines are the intersections of the surfaces

$$f(\rho,\theta,\phi) = \text{constant} \tag{7}$$

and

$$u = A_1 x + A_2 y + A_3 z = \text{constant}. \tag{8}$$

The generating function $f(\rho,\theta,\phi)$ determines the magnetic surfaces of the stationary electromagnetic waves. For the different eigenmodes, the field lines are the intersections of these surfaces with the x, y, or z = constant planes. The eigenmodes can be defined also as a superposition of the eigenmodes introduced by us, and, in this case, the magnetic field lines can be obtained again through the intersection of the magnetic surfaces (7) with the corresponding surfaces. The magnetic surfaces are given in Fig. 1 for the most characteristic cases if the generating function has the form [3]

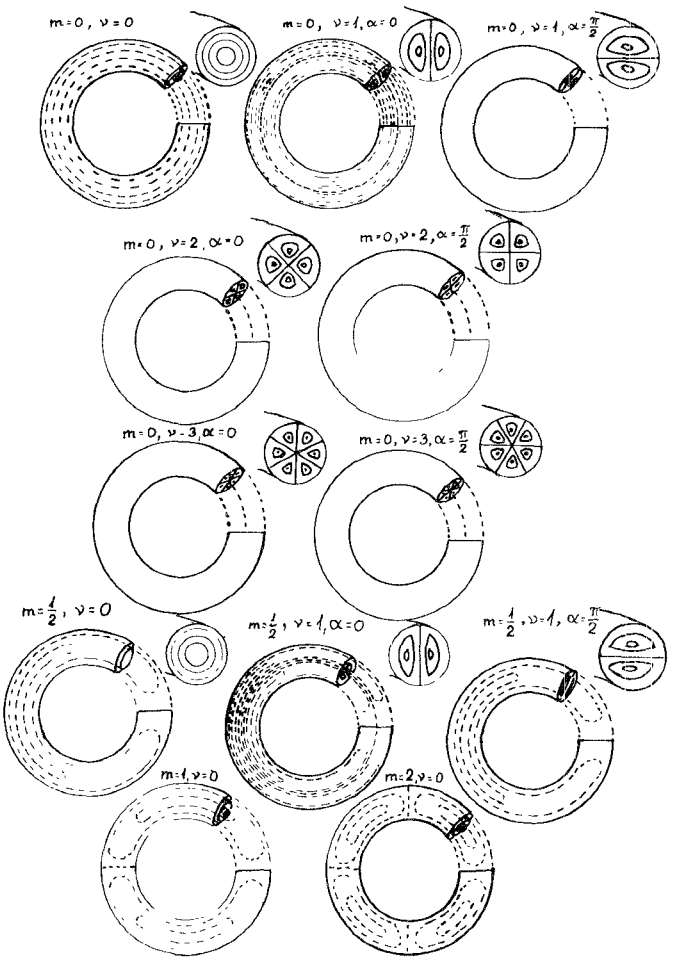

Fig. 1. Magnetic surfaces of toroidal electromagnetic modes for an empty torus.

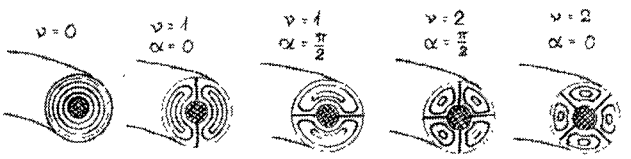

Fig. 2. Magnetic surfaces of toroidal electromagnetic modes for coaxial toroidal systems.

$$f(\rho,\theta,\phi) = \frac{Z_\nu(k\rho)}{\sqrt{1-\rho\cos\theta}}\cos(\nu\theta-\alpha)\sin m\phi. \tag{9}$$

Here, ν is an integer, $m = 0, 1/2, 1, 2, 3, \cdots, \alpha = 0$ or $\pi/2$, and $Z_\nu(k\rho)$ is a cylindrical function. Fig. 1 corresponds to the case of the empty torus. In this case, $Z_\nu(k\rho)$ is the Bessel function $J_\nu(k\rho)$. If we consider the case of a coaxial torus, or of a torus containing an isotropic plasma, which is separated from the wall by means of a magnetic field, the function $Z_\nu(k\rho)$ will be a superposition of the Bessel and Neumann functions $Z_\nu(k\rho) = C_1 J_\nu(k\rho) + C_2 N_\nu(k\rho)$. The ϕ = constant sections of the corresponding magnetic surfaces are represented in Fig. 2.

III. Stationary Waves with Periodicity of 4π

For toroidal systems with a periodicity of 4π (torus with separating wall (See Fig. 3)), the possibility appears to get an exact solution of the Maxwell equations for the stationary waves. This solution can be obtained if we use the following generating function for the construction of the Hertz vector:

$$f=\frac{Z_\nu(k\rho)}{\sqrt{1-\rho\cos\theta}}\cos(\nu\theta-\alpha)\sin\frac{\phi}{2}. \tag{10}$$

This function is an exact solution of the scalar Helmholtz equation in toroidal coordinates. Here

$$k=\frac{\omega R}{c} \tag{11}$$

where R is the major radius of the torus, ω is the eigenfrequency of the wave, and c is the speed of light. Here, it is assumed that the toroidal coordinate ρ is equal to the ratio r/R of the minor radius of a given point and the major radius of the torus.

Using the generating function (10), we can construct the toroidal components of the Hertz vector. We shall study two types of normal modes:

$$1)\ \vec{P}=\vec{P}(f\sin\theta, f\cos\theta, 0) \tag{12}$$

$$2)\ \vec{P}=\vec{P}(-f\cos\theta\cos\phi, f\sin\theta\cos\phi, -f\sin\phi). \tag{13}$$

The third normal mode, corresponding to $\vec{P}^b$ (see (3)) differs from (13) only by a rotation through $\pi/2$ around the axis of the torus.

A. The Intensity of the Magnetic Field

Using (1), we get the following for the two types of normal modes.

1) Normal Modes of the First Type:

$$B_\rho\sim-\frac{Z_\nu(k\rho)}{\sqrt{(1-\rho\cos\theta)^3}}\cos(\nu\theta-\alpha)\cos\theta\cos\frac{\phi}{2} \tag{14}$$

$$B_\theta\sim\frac{Z_\nu(k\rho)}{\sqrt{(1-\rho\cos\theta)^3}}\cos(\nu\theta-\alpha)\sin\theta\cos\frac{\phi}{2} \tag{15}$$

$$B_\phi\sim\frac{Z_\nu(k\rho)}{2\sqrt{(1-\rho\cos\theta)^3}}\left\{\cos(\nu\theta-\alpha)+\frac{2\nu}{\rho}(1-\rho\cos\theta)\cdot\cos\left[(\nu-1)\theta-\alpha\right]\right\}\sin\frac{\phi}{2}$$
$$-\frac{kZ_{\nu+1}(k\rho)}{\sqrt{1-\rho\cos\theta}}\cos(\nu\theta-\alpha)\cos\theta\sin\frac{\phi}{2}. \tag{16}$$

The magnetic field lines are the intersections of

$$\frac{Z_\nu(k\rho)}{\sqrt{1-\rho\cos\theta}}\cos(\nu\theta-\alpha)\sin\frac{\phi}{2}=\text{constant} \tag{17}$$

and the $z=$constant plane.

2) Normal Modes of the Second Type:

$$B_\rho\sim\frac{\nu Z_\nu(k\rho)}{\rho\sqrt{1-\rho\cos\theta}}\sin(\nu\theta-\alpha)\sin\phi\sin\frac{\phi}{2}$$
$$-\frac{Z_\nu(k\rho)}{2\sqrt{(1-\rho\cos\theta)^3}}\sin\theta\cos(\nu\theta-\alpha)\cos\frac{3\phi}{2} \tag{18}$$

$$B_\theta\sim\left[\frac{\nu Z_\nu(k\rho)}{\rho\sqrt{1-\rho\cos\theta}}-\frac{kZ_{\nu+1}(k\rho)}{\sqrt{1-\rho\cos\theta}}\right]\cdot\cos(\nu\theta-\alpha)\sin\phi\sin\frac{\phi}{2}$$
$$-\frac{Z_\nu(k\rho)}{2\sqrt{(1-\rho\cos\theta)^3}}\cos\theta\cos(\nu\theta-\alpha)\cos\frac{3\phi}{2} \tag{19}$$

$$B_\phi\sim-\frac{kZ_{\nu+1}(k\rho)}{\sqrt{1-\rho\cos\theta}}\sin\theta\cos(\nu\theta-\alpha)\cos\phi\sin\frac{\phi}{2}$$
$$-\frac{\nu Z_\nu(k\rho)}{\rho\sqrt{1-\rho\cos\theta}}\sin\left[(\nu-1)\theta-\alpha\right]\cos\phi\sin\frac{\phi}{2}. \tag{20}$$

The magnetic field lines are the intersections of the surfaces (17) with the $x=$constant plane. The structure of the magnetic surfaces can be seen in Figs. 1 and 2.

B. The Boundary Conditions

At the conducting surface, the normal component of the magnetic field must vanish. This is realized if

$$Z_\nu(k\rho)=0 \tag{21}$$

at the surface of the torus. Simultaneously, the ϕ-component of $\vec{B}$ must vanish at the conducting separating wall. The generating function (10) was chosen in such a manner that this is automatically fulfilled for the plane

$$\phi=0. \tag{22}$$

C. The Dispersion Relation

1) Empty Toroidal Resonator with a Separating Wall: Inside the empty torus, the electromagnetic field cannot have any singularities. Therefore, the cylindrical function $Z_\nu(k\rho)$ must be the Bessel function $J_\nu(k\rho)$, and the condition (21) leads to

$$J_\nu(k\rho_0)=0 \tag{23}$$

where ρ_0 is the inverse aspect ratio of the torus. Condition (23) means that

$$k\rho_0=j_{\nu,1} \tag{24}$$

where $j_{\nu,1}$ is the first root of the Bessel function J_ν. Using (11), (24), and the definition of the inverse aspect ratio $\rho_0=r_0/R$, we get for the dispersion relation

$$\boxed{\omega_\nu=\frac{c}{r_0}j_{\nu,1}}. \tag{25}$$

Therefore, the eigenfrequency of the resonator depends

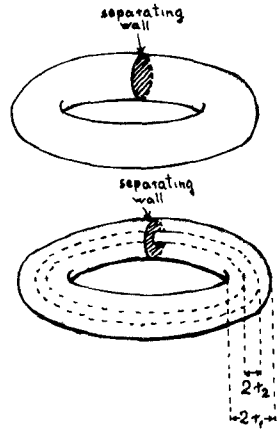

Fig. 3. Toroidal resonators with separating wall.

only on the minor radius of the torus. This is a direct consequence of the existence of $B_\rho = 0$ nodes at the toroidal surface. For the associated wavelength in free vacuum, we get $\lambda_\nu = 2\pi r_0 / j_{\nu,1}$.

2) Coaxial Toroidal Resonator with a Separating Wall: In the case of the coaxial toroidal resonator, condition (21) must be fulfilled for the outer torus ($r = r_1$) and for the inner torus ($r = r_2$). We must take Z_ν as a superposition of the Bessel and Neumann functions and for the dispersion relation results:

$$\boxed{\omega_\nu = \frac{c}{r_1} a_{\nu,1}} \tag{26}$$

where $a_{\nu,1}$ is the first root of the equation

$$N_\nu(a) J_\nu\left(\frac{r_1 a}{r_2}\right) - N_\nu\left(\frac{r_1 a}{r_2}\right) J_\nu(a) = 0. \tag{27}$$

(The numerical values of $j_{\nu,1}$ and $a_{\nu,1}$ are given, e.g., in [4].)

D. The Intensity of the Electric Field

The intensity of the electric field can be determined by the well-known relation

$$\vec{E} = k^2 \vec{P} + \text{grad div } \vec{P}. \tag{28}$$

For the toroidal components of the intensity, we get the following.

1) Normal Modes of the First Type:

$$\begin{aligned} E_\rho = &- \frac{\nu(\nu-1) Z_\nu(k\rho)}{\rho^2 \sqrt{1-\rho\cos\theta}} \sin\left[(\nu-1)\theta - \alpha\right] \sin\frac{\phi}{2} \\ &- \frac{\nu Z_\nu(k\rho)}{2\rho\sqrt{(1-\rho\cos\theta)^3}} \sin\left[(\nu-1)\theta - \alpha\right] \cos\theta \sin\frac{\phi}{2} \\ &+ \frac{k Z_{\nu+1}(k\rho)}{2\rho\sqrt{(1-\rho\cos\theta)^3}} (2 - 3\rho\cos\theta) \\ &\cdot \cos(\nu\theta - \alpha) \sin\theta \sin\frac{\phi}{2} \\ &+ \frac{\nu k Z_{\nu+1}(k\rho)}{\rho\sqrt{1-\rho\cos\theta}} \sin(\nu\theta - \alpha) \cos\theta \sin\frac{\phi}{2} \end{aligned} \tag{29}$$

$$\begin{aligned} E_\theta = &\frac{k^2 Z_\nu(k\rho)}{\sqrt{1-\rho\cos\theta}} \cos(\nu\theta - \alpha) \cos\theta \sin\frac{\phi}{2} \\ &+ \frac{\nu Z_\nu(k\rho)}{2\rho\sqrt{(1-\rho\cos\theta)^3}} \sin\left[(\nu-1)\theta - \alpha\right] \sin\theta \sin\frac{\phi}{2} \\ &- \frac{\nu(\nu-1) Z_\nu(k\rho)}{\rho^2\sqrt{1-\rho\cos\theta}} \cos\left[(\nu-1)\theta - \alpha\right] \sin\frac{\phi}{2} \\ &- \frac{k Z_{\nu+1}(k\rho)}{\rho\sqrt{1-\rho\cos\theta}} \cos(\nu\theta - \alpha) \cos\theta \sin\frac{\phi}{2} \\ &+ \frac{\nu k Z_{\nu+1}(k\rho)}{\rho\sqrt{1-\rho\cos\theta}} \sin(\nu\theta - \alpha) \sin\theta \sin\frac{\phi}{2} \\ &+ \frac{k Z_{\nu+1}(k\rho)}{2\sqrt{(1-\rho\cos\theta)^3}} \sin^2\theta \cos(\nu\theta - \alpha) \sin\frac{\phi}{2} \end{aligned} \tag{30}$$

$$\begin{aligned} E_\phi = &- \frac{\cos\frac{\phi}{2}}{2\rho\sqrt{(1-\rho\cos\theta)^3}} \\ &\cdot \left\{\nu Z_\nu(k\rho) \sin\left[(\nu-1)\theta - \alpha\right]\right. \\ &\left. + k\rho Z_{\nu+1}(k\rho) \cos(\nu\theta - \alpha) \sin\theta\right\} \end{aligned} \tag{31}$$

2) Normal Modes of the Second Type:

$$\begin{aligned} E_\rho = &- \left(\frac{3}{4} \frac{Z_\nu(k\rho)}{\sqrt{(1-\rho\cos\theta)^5}} \cos\theta + \frac{\nu Z_\nu(k\rho)}{2\rho\sqrt{(1-\rho\cos\theta)^3}}\right) \\ &\cdot \cos(\nu\theta - \alpha) \sin\frac{3\phi}{2} \\ &+ \left(\frac{\nu Z_\nu(k\rho)}{\rho^2\sqrt{1-\rho\cos\theta}} - \frac{\nu Z_\nu(k\rho)}{2\rho\sqrt{(1-\rho\cos\theta)^3}} \cos\theta\right. \\ &\left. - \frac{\nu^2 Z_\nu(k\rho)}{\rho^2\sqrt{1-\rho\cos\theta}}\right) \cos\left[(\nu-1)\theta - \alpha\right] \cos\phi \sin\frac{\phi}{2} \\ &+ \left(\frac{k}{2} \frac{Z_{\nu+1}(k\rho)}{\sqrt{(1-\rho\cos\theta)^3}} \cos\theta - \frac{k(\nu+1) Z_{\nu+1}(k\rho)}{\rho\sqrt{1-\rho\cos\theta}}\right) \\ &\cdot \cos(\nu\theta - \alpha) \cos\theta \cos\phi \sin\frac{\phi}{2} \\ &+ \frac{k Z_{\nu+1}(k\rho)}{2\sqrt{(1-\rho\cos\theta)^3}} \cos(\nu\theta - \alpha) \sin\frac{3\phi}{2} \\ &+ \frac{k\nu Z_{\nu+1}(k\rho)}{\rho\sqrt{1-\rho\cos\theta}} \cos\left[(\nu-1)\theta - \alpha\right] \cos\phi \sin\frac{\phi}{2} \end{aligned} \tag{32}$$

$$E_\theta = k^2 \frac{Z_\nu(k\rho)}{\sqrt{1-\rho\cos\theta}} \cos(\nu\theta-\alpha)\sin\theta\cos\phi\sin\frac{\phi}{2}$$
$$+\frac{3Z_\nu(k\rho)}{4\sqrt{(1-\rho\cos\theta)^5}}\cos(\nu\theta-\alpha)\sin\theta\sin\frac{3\phi}{2}$$
$$+\frac{\nu Z_\nu(k\rho)}{2\rho\sqrt{(1-\rho\cos\theta)^3}}\left\{\sin(\nu\theta-\alpha)\sin\frac{3\phi}{2}\right.$$
$$\left.+\cos\left[(\nu-1)\theta-\alpha\right]\sin\theta\cos\phi\sin\frac{\phi}{2}\right\}$$
$$+\frac{\nu(\nu-1)Z_\nu(k\rho)}{\rho^2\sqrt{1-\rho\cos\theta}}\sin\left[(\nu-1)\theta-\alpha\right]\cos\phi\sin\frac{\phi}{2}$$
$$-\frac{kZ_{\nu+1}(k\rho)}{2\rho\sqrt{(1-\rho\cos\theta)^3}}\cos(\nu\theta-\alpha)\cos\theta$$
$$\cdot\sin\theta\cos\phi\sin\frac{\phi}{2}$$
$$-\frac{k\nu Z_{\nu+1}(k\rho)}{\rho\sqrt{1-\rho\cos\theta}}\sin(\nu\theta-\alpha)\cos\theta\cos\phi\sin\frac{\phi}{2}$$
$$-\frac{kZ_{\nu+1}(k\rho)}{\rho\sqrt{1-\rho\cos\theta}}\cos(\nu\theta-\alpha)\sin\theta\cos\phi\sin\frac{\phi}{2} \tag{33}$$

$$E_\phi = -\frac{k^2 Z_\nu(k\rho)}{\sqrt{1-\rho\cos\theta}}\cos(\nu\theta-\alpha)\sin\phi\sin\frac{\phi}{2}$$
$$-\frac{3Z_\nu(k\rho)}{4\sqrt{(1-\rho\cos\theta)^5}}\cos(\nu\theta-\alpha)\cos\frac{3\phi}{2}$$
$$-\frac{\nu Z_\nu(k\rho)}{2\rho\sqrt{(1-\rho\cos\theta)^3}}\cos\left[(\nu-1)\theta-\alpha\right]\cos\phi\cos\frac{\phi}{2}$$
$$+\frac{\nu Z_\nu(k\rho)}{\rho\sqrt{(1-\rho\cos\theta)^3}}\cos\left[(\nu-1)\theta-\alpha\right]\sin\phi\sin\frac{\phi}{2}$$
$$-\frac{kZ_{\nu+1}(k\rho)}{\sqrt{(1-\rho\cos\theta)^3}}\cos(\nu\theta-\alpha)\cos\theta\sin\phi\sin\frac{\phi}{2}$$
$$+\frac{kZ_{\nu+1}(k\rho)}{2\sqrt{(1-\rho\cos\theta)^3}}\cos(\nu\theta-\alpha)\cos\theta\cos\frac{\phi}{2}\cos\phi. \tag{34}$$

E. The Charge Density at the Toroidal Surface

The charge density at the toroidal surface is proportional to the normal component of the electric field's intensity. Taking into account the boundary condition (21), we get the following.

1) For the modes of the first type from (29),

$$\sigma\sim\frac{2-3\rho\cos\theta}{2\sqrt{(1-\rho\cos\theta)^3}}\cos(\nu\theta-\alpha)\sin\theta\sin\frac{\phi}{2}$$
$$+\frac{\nu}{\sqrt{1-\rho\cos\theta}}\sin(\nu\theta-\alpha)\cos\theta\sin\frac{\phi}{2}. \tag{35}$$

2) For the modes of the second type from (32),

$$\sigma\sim-\frac{2(\nu+1)-(2\nu+3)\rho\cos\theta}{\sqrt{(1-\rho\cos\theta)^3}}$$
$$\cdot\cos(\nu\theta-\alpha)\cos\theta\cos\phi\sin\frac{\phi}{2}$$
$$+\frac{\rho}{\sqrt{(1-\rho\cos\theta)^3}}\cos(\nu\theta-\alpha)\sin\frac{3\phi}{2}$$
$$+\frac{2\nu}{\sqrt{1-\rho\cos\theta}}\cos\left[(\nu-1)\theta-\alpha\right]\cos\phi\sin\frac{\phi}{2}. \tag{36}$$

As can be seen, the charge density profile at the toroidal surface does not depend on the cylindrical function. Therefore, it is the same for empty toroidal resonators and for the coaxial toroidal resonators (or for resonators containing plasma). In the case of the coaxial toroidal resonators, (35) and (36) can also be used for the surface of the inner torus, however, with the opposite sign.

The charge density on the separating wall is always proportional to E_ϕ.

IV. Particular Examples for Toroidal Modes with Periodicity 4π

A. Normal Modes of the First Type

1) $\nu=0$: For the charge density on the surface of the torus results:

$$\sigma\sim\frac{2-3\rho\cos\theta}{2\sqrt{(1-\rho\cos\theta)^3}}\cos\alpha\sin\theta\sin\frac{\phi}{2}. \tag{37}$$

For the charge density on the separating wall, we get from (31)

$$\sigma_{sep}\sim-\frac{Z_{\nu+1}(k\rho)}{\sqrt{(1-\rho\cos\theta)^3}}\cos\alpha\sin\theta. \tag{38}$$

It can be seen that only the $\alpha=0$ mode exists. (The charge densities and the field intensities both vanish for $\alpha=\pi/2$.)

The charge distribution and the corresponding electric and magnetic field lines are given for the empty torus in Fig. 4. The magnetic field lines are the intersections of the surfaces $(1-\rho\cos\theta)^{-1/2}Z_0(k\rho)\sin(\phi/2)=$ constant and $z=$ constant.

As it can be seen in the figure, there is a dipole oscillation of the charge density on the separating wall.

2) $\nu=1$: For the charge densities on the surface of the torus and on the separating wall results:

$$\sigma\sim\frac{2-3\rho\cos\theta}{2\sqrt{(1-\rho\cos\theta)^3}}\sin\theta\cos(\theta-\alpha)\sin\frac{\phi}{2}$$
$$+\frac{1}{\sqrt{1-\rho\cos\theta}}\sin(\theta-\alpha)\cos\theta\sin\frac{\phi}{2} \tag{39}$$

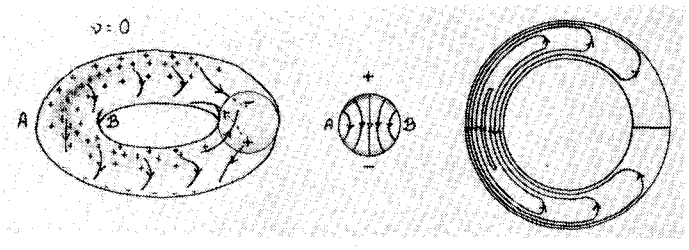

Fig. 4. Surface charge distribution and field structure of the normal modes of the first type for $\nu=0$.

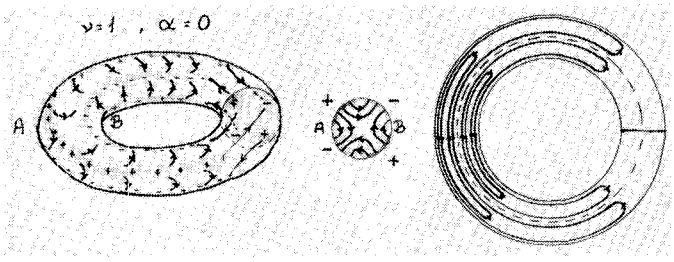

Fig. 5. Surface charge distribution and field structure of the normal modes of the first type for $\nu=1$ and $\alpha=0$.

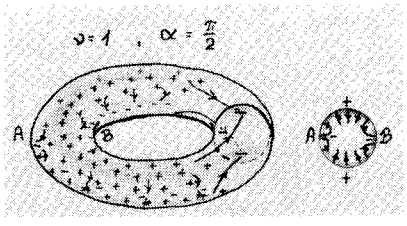

Fig. 6. Surface charge distribution and field structure of the normal modes of the first type for $\nu=1$ and $\alpha=\pi/2$.

$$\sigma_{\text{sep}} \sim -\frac{1}{2\rho\sqrt{(1-\rho\cos\theta)^3}} \cdot \{k\rho Z_2(k\rho)\cos(\theta-\alpha)\sin\theta - Z_1(k\rho)\sin\alpha\}. \quad (40)$$

The distribution of the electric charges and the electric field lines are represented in Fig. 5 for $\alpha=0$ and in Fig. 6 for $\alpha=\pi/2$.

It can be seen that, for $\nu=1$, $\alpha=0$, we have a quadrupole oscillation of charge on the separating wall. For this case, we have also represented the magnetic field lines.

B. *Normal Modes of the Second Type*

1) $\nu=0$*:* The charge densities are

$$\sigma \sim -\frac{2-3\rho\cos\theta}{\sqrt{(1-\rho\cos\theta)^3}}\cos\alpha\cos\theta\cos\phi\sin\frac{\phi}{2} + \frac{\rho}{\sqrt{(1-\rho\cos\theta)^3}}\cos\alpha\sin\frac{3\phi}{2} \quad (41)$$

$$\sigma_{\text{sep}} \sim -\frac{3Z_0(k\rho)}{4\sqrt{(1-\rho\cos\theta)^5}}\cos\alpha + \frac{kZ_1(k\rho)}{2\sqrt{(1-\rho\cos\theta)^3}}\cos\alpha\cos\theta. \quad (42)$$

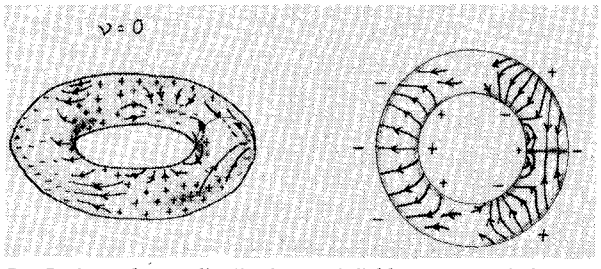

Fig. 7. Surface charge distribution and field structure of the normal modes of the second type for $\nu=0$.

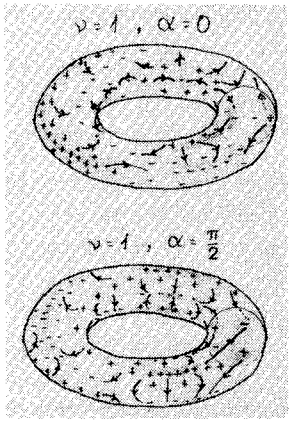

Fig. 8. Surface charge distribution and field structure of the normal modes of the second type for $\nu=1$.

Here, we have again only the mode $\alpha=0$. The electric charge densities and the field lines are represented in Fig. 7. There is again a dipole oscillation of the charge density on the separating wall. The oscillation is now in the direction of the major radius of the torus. Therefore, as a consequence of the curvature of the torus, an asymmetry in the dipole charge distribution appears.

2) $\nu=1$*:* For the charge densities, we have

$$\sigma \sim -\frac{4-5\rho\cos\theta}{\sqrt{(1-\rho\cos\theta)^3}}\cos(\theta-\alpha)\cos\theta\cos\phi\sin\frac{\phi}{2} + \frac{\rho}{\sqrt{(1-\rho\cos\theta)^3}}\sin\frac{3\phi}{2}\cos(\theta-\alpha) + \frac{2\cos\alpha}{\sqrt{1-\rho\cos\theta}}\cos\phi\sin\frac{\phi}{2} \quad (43)$$

$$\sigma_{\text{sep},\alpha=0} \sim -\frac{3Z_1(k\rho)}{4\sqrt{(1-\rho\cos\theta)^5}}\cos\theta - \frac{Z_1(k\rho)}{2\rho\sqrt{(1-\rho\cos\theta)^3}} + \frac{kZ_2(k\rho)}{2\sqrt{(1-\rho\cos\theta)^3}}\cos^2\theta \quad (44)$$

$$\sigma_{\text{sep},\alpha=\pi/2} \sim -\frac{3Z_1(k\rho)}{4\sqrt{(1-\rho\cos\theta)^5}}\sin\theta + \frac{kZ_2(k\rho)}{4\sqrt{(1-\rho\cos\theta)^3}}\sin 2\theta. \quad (45)$$

The charge densities and the electric field lines are represented in Fig. 8. As can be seen, in the case of the second-type modes, we also get a quasi-quadrupole oscillation on the separating wall. Here, again, the influence of the curvature of the torus appears.

V. Conclusions

The paper contains the solution of Maxwell's equations for a torus with a separating wall. We think that the great advantage of the described solution is that it is an exact one for a complicated geometry, and no approximations were used anywhere.

The special symmetry of the torus with a separating wall does not allow the simple E and H classification of the waves. Therefore, we had to introduce a different classification, which was dictated by our mathematical method.

Acknowledgment

The author acknowledges the support by the Österreichischer Fonds zur Förderung der wissenschaftlichen Forschung. He would also like to express his gratitude to Prof. F. Cap for useful discussions during the elaboration of this paper.

References

[1] F. Cap and R. Deutsch, "Toroidal electromagnetic modes in isotropic homogeneous plasma and in vacuum," presented at the 3rd Int. Congress on Waves and Instabilities in Plasmas, Paris, France, June 27–July 2, 1977.

[2] ——, "Toroidal resonators for electromagnetic waves," *IEEE Trans. Microwave Theory Tech.*, vol. MTT-26, pp. 478–486, July 1978.

[3] R. Deutsch, "Toroidal electromagnetic modes in a torus containing plasma and in coaxial toroidal systems," to be published.

[4] Jahnke, Emde, and Lösch, *Tables of Higher Functions*. Stuttgart, Germany: B. G. Teubner Verlagsgesellschaft, 1960.

Characteristics and Optimum Operating Parameters of a Gyrotron Traveling Wave Amplifier

KWO RAY CHU, ADAM T. DROBOT, VICTOR L. GRANATSTEIN, AND J. LARRY SEFTOR

Abstract—**Characteristics and optimum operating parameters are determined for a new type of high-power high-efficiency generator of millimeter waves known as a gyrotron traveling wave amplifier. In the example considered, wave amplification results from the interaction of a TE_{01} waveguide mode with the fundamental cyclotron harmonic of an electron beam. The parameter optimization involves the determination of the point of maximum device efficiency as a function of beam density, beam energy, beam positioning, and external magnetic field for the output power required. An analytical linear theory and a numerical simulation code form the basis of theoretical calculations. As a result of the extensive survey in parameter space, the peak efficiency in the beam frame has been found to exceed 70 percent. This result has been applied to the specific design of a 35-GHz amplifier with output power ~340 kW, a power gain of 2 dB/cm, and a laboratory frame efficiency of 51 percent.**

Manuscript received October 7, 1977; revised May 11, 1978. This work was supported in part by the Naval Electronic Systems Command, Task XF 54-587, by the Army Ballistic Missile Defense Advanced Technology Center, MIPR W31RPD-73-Z787, and by the Naval Surface Weapons Center (Dahlgren), Task SF32-302-41B.

K. R. Chu was with Science Applications, Inc., McLean, VA. He is now with the Plasma Physics Division, Naval Research Laboratory, Washington, DC 20375.

A. T. Drobot is with Science Applications, Inc., McLean, VA 22101.

V. L. Granatstein and J. L. Seftor are with the Plasma Physics Division, Naval Research Laboratory, Washington, DC 20375.

I. Introduction

THE GYROTRON is a new type of microwave device employing the electron cyclotron maser mechanism. It ideally consists of an ensemble of monoenergetic electrons following helical trajectories around the lines of an axial magnetic field inside a fast wave structure such as a metallic tube or waveguide. The physical mechanism responsible for the radiation in the gyrotrons has its origin in a relativistic effect. Initially, the phases of the electrons in their cyclotron orbits are random, but phase bunching can occur because of the dependence of electron cyclotron frequency on the relativistic electron mass. Those electrons that lose energy to the wave become lighter, rotate faster, and, hence, accumulate phase lead, while those electrons that gain energy from the wave become heavier, rotate slower, and accumulate phase lag. This can result in phase bunching such that the electrons radiate coherently and amplify the wave. Energy transfer from the electrons to the wave is optimized when $\omega - k_z v_{z0} - s\Omega_c \geqslant 0$, where ω, k_z, v_{z0}, s, and Ω_c, are, respectively, the wave frequency, axial wave number, axial electron veloc-

0018-9480/79/0200-0178$00.75 ©1979 IEEE